Reaching During Virtual Rotation: Context Specific Compensations for Expected Coriolis Forces

JOSEPH V. COHN, PAUL DiZIO, AND JAMES R. LACKNER
Ashton Graybiel Spatial Orientation Laboratory and Volen Center for Complex Systems, Brandeis University, Waltham, Massachusetts 02454-9110

Cohn, Joseph V., Paul DiZio, and James R. Lackner. Reaching during virtual rotation: context specific compensations for expected Coriolis forces. *J Neurophysiol* 83: 3230–3240, 2000. Subjects who are in an enclosed chamber rotating at constant velocity feel physically stationary but make errors when pointing to targets. Reaching paths and endpoints are deviated in the direction of the transient inertial Coriolis forces generated by their arm movements. By contrast, reaching movements made during natural, voluntary torso rotation seem to be accurate, and subjects are unaware of the Coriolis forces generated by their movements. This pattern suggests that the motor plan for reaching movements uses a representation of body motion to prepare compensations for impending self-generated accelerative loads on the arm. If so, stationary subjects who are experiencing illusory self-rotation should make reaching errors when pointing to a target. These errors should be in the direction opposite the Coriolis accelerations their arm movements would generate if they were actually rotating. To determine whether such compensations exist, we had subjects in four experiments make visually open-loop reaches to targets while they were experiencing compelling illusory self-rotation and displacement induced by rotation of a complex, natural visual scene. The paths and endpoints of their initial reaching movements were significantly displaced leftward during counterclockwise illusory rotary displacement and rightward during clockwise illusory self-displacement. Subjects reached in a curvilinear path to the wrong place. These reaching errors were opposite in direction to the Coriolis forces that would have been generated by their arm movements during actual torso rotation. The magnitude of path curvature and endpoint errors increased as the speed of illusory self-rotation increased. In successive reaches, movement paths became straighter and endpoints more accurate despite the absence of visual error feedback or tactile feedback about target location. When subjects were again presented a stationary scene, their initial reaches were indistinguishable from pre-exposure baseline, indicating a total absence of aftereffects. These experiments demonstrate that the nervous system automatically compensates in a context-specific fashion for the Coriolis forces associated with reaching movements.

INTRODUCTION

When we reach for an object while simultaneously rotating our torso, our moving arm generates an inertial force known as the Coriolis force. A Coriolis force arises in a rotating system whenever a body revolving with the system moves nonparallel to the axis of rotation. We shall show that in turning and reaching maneuvers the CNS registers body velocity and automatically precompensates for the Coriolis forces that will be generated after the arm starts moving. This automatic compensation is why during our everyday activities we can execute reaching movements as desired and be unaware of the Coriolis forces that are a consequence of our own body movements.

The Coriolis force (F_{Cor}) on a moving object in a rotating frame of reference is a function of the object's mass, m, and the cross product of the frame's angular velocity, $\vec{\omega}$, and the object's linear velocity, $\vec{v}$, relative to the reference frame: $F_{\mathrm{cor}} = -2m(\vec{\omega} \times \vec{v})$. The Coriolis force always acts orthogonal to the movement path. In a room rotating counterclockwise (CCW), an object moving away from an observer will be deviated rightward, and in a room rotating clockwise (CW) it will be deviated leftward.

Lackner and DiZio (1994) have studied the effects of Coriolis forces on the reaching movements of subjects passively exposed to rotation within a fully enclosed slow rotation room (SRR). The SRR was accelerated slowly to 60°/s, CCW velocity, with subjects seated at the center. The subjects always felt completely stationary during the experiment. The centrifugal force due to rotation was negligible, producing a gravitoinertial resultant force just 0.006% above the normal 1.0 g background. This means that except when subjects made a reaching movement, the forces acting on their body were the same as without rotation. But, when subjects reached to point at a target, their forward-moving arm generated a rightward Coriolis force, the magnitude of which depended on the linear velocity of the reaching arm. Because hand velocity in a typical reaching movement follows a bell-shaped profile (Morasso 1981), the magnitude of the Coriolis force also varied in the same manner. At 60°/s, the peak Coriolis force generated by the arm movements ranged between 0.1 and 0.3 g.[1] All of the subjects tested showed large movement trajectory deviations and missed the target.

The pattern of errors was very consistent. As the forward velocity of the arm increased, the arm became progressively deviated rightward in the direction of the Coriolis force. This trajectory deviation then diminished somewhat as the arm velocity and Coriolis force abated. When the movement was over, the end position of the pointing hand remained significantly deviated to the right side of the target. This pattern was seen in the initial reaches of every subject. Subjects, as they reached, felt that their arm did not follow its intended path, that "something" had forced it to the side even though they felt no mechanical contact or interference.

The subjects in these experiments received neither visual nor

The costs of publication of this article were defrayed in part by the payment of page charges. The article must therefore be hereby marked "*advertisement*" in accordance with 18 U.S.C. Section 1734 solely to indicate this fact.

[1] We will use the symbol g as a unit of "force," although it technically denotes force per unit mass in multiples of Earth's gravitational acceleration, ~9.8 m/s^2.

direct tactile feedback concerning their movement errors. Nevertheless, with additional reaches during rotation, their movements became increasingly more accurate, showing progressively straighter paths and less deviated endpoints. Within ~10 to 15 movements, each subject returned to prerotation baseline performance. As subjects regained their straight and accurate reaching paths, their reaches again felt normal. The transient Coriolis forces generated by their arm movements were no longer perceived, although they were still present. After the slow rotation room was brought to a stop (at a rate below threshold for perception of motion), the subjects made additional reaches to the target. The initial postrotation reaches of all subjects were (viewed from above) mirror images of their initial reaches made during rotation. Every subject reported that it felt as if an external force had deviated their arm left of its intended path. With repeated reaches, their movements returned to prerotation baseline patterns, and they no longer experienced an "alien force" deviating their arm from its intended path. Every subject also reported feeling stationary throughout the entire experiment.

It is important to recognize that compensation for Coriolis forces is also important in a normal environment where the torso is free to move when we reach. In natural turning and reaching, the torso becomes a rotating reference frame for the moving arm. Consequently, when the arm is projected outward, it undergoes a substantial lateral Coriolis force. Figure 1 presents experimental measurements of lateral hand acceleration for three torso rotation conditions in which forward hand velocity is nearly the same.

The *left-most traces* are for a seated, stationary subject; only small lateral acceleration is present. The *middle traces* were recorded from a subject seated in a slow rotation room that was turning at 60°/s constant velocity. The lateral acceleration generated on the hand is nearly 0.25 *g*, and the subject will misreach in a curvilinear path. The traces on the *right* are from a standing subject who makes a natural turning and reaching movement. The peak angular velocity of the torso reaches 365°/s, and the lateral acceleration on the hand is nearly 0.5 *g*. Nevertheless, the subject

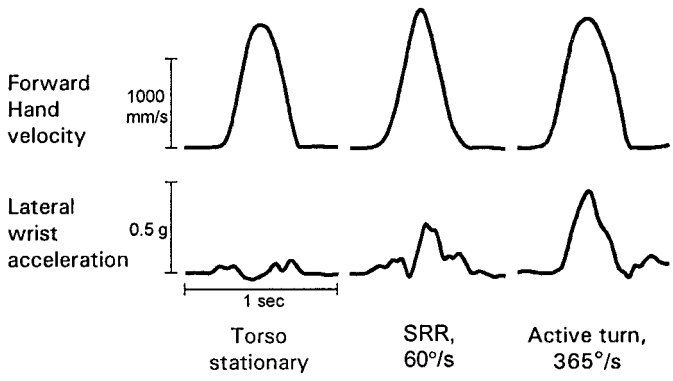

FIG. 1. Comparison of lateral accelerations of the wrist (*bottom*, recorded with an accelerometer) produced when the hand moves forward relative to the torso at roughly the same velocities (*top*, recorded photogramatically) in 3 different torso motion conditions. *Left*: torso stationary in a normal environment. Small magnitude oscillations of lateral acceleration occur. *Middle*: subject seated in a rotating room turning at 60°/s. The lateral acceleration profile is bell-shaped, like hand velocity, peaking at ~0.25*g*. *Right*: voluntary torso rotation (peak angular velocity 365°/s, measured with a rate sensor) while reaching forward in a normal environment. The lateral acceleration, a combination of Coriolis force and tangential acceleration due to angular acceleration of the torso, has a bell-shaped profile peaking at ~0.5*g*.

is able to reach accurately (Pigeon et al. 1999). Inverse dynamics computations show that Coriolis joint torques are substantial in such active turning and reaching and allow precise assessments of their magnitude (Bortolami et al. 1999). The Coriolis forces generated by reaching movements during active turning are large, yet they are not perceived. By contrast, in the slow rotation room the Coriolis forces generated by comparable velocity reaching movements are only half as large but are perceived as very substantial and disrupt movement path and accuracy. This pattern suggests that our nervous system normally compensates for self-generated Coriolis forces in planning movements to guide them appropriately and maintains these compensations perceptually transparent.

Our goals in the present paper have been to obtain experimental proof that Coriolis forces associated with self-motion are automatically offset and to gain insight into how the nervous system does this. Our approach was to use visual stimulation to induce the nervous system into registering that the body was rotating and that compensations for Coriolis forces were necessary when they actually were not. Then, by examining the resulting in vacuo reactions as reflected in perturbations of movement paths, we could see the time course and pattern of the compensatory process in action.

We induced apparent body rotation using a head-mounted device (HMD) that displayed stereoscopic video images transmitted from a pair of cameras on a turntable in the center of a cluttered laboratory room. Our display also presented a virtual stationary surface containing targets that subjects pointed to. The subject's arms, were concealed by the HMD, precluding visual feedback about hand position and pointing accuracy. Howard and Childerson (1994) have shown that a rotating scene containing distinctive, polarized objects is more effective than abstract, periodic, or random patterns for inducing illusions of self-displacement. Although natural turning and reaching movements provide multisensory and efferent cues about rotation, we predicted that a powerful visual stimulus alone would be sufficient for Coriolis compensations to occur.

With actual voluntary rotation to the left, CCW, the Coriolis force generated by a forward reaching movement would act rightward; therefore a subject would have to compensate leftward to achieve the desired movement path. Therefore, if a stationary subject experiencing compelling illusory, CCW self-rotation exhibited compensation for the anticipated Coriolis force associated with rotation, we would expect him or her to reach too far to the left when attempting to point to targets. We would also expect the path of a movement to be curvilinear, initially deviating to the left and then returning a fraction of the initial deviation toward the right. The opposite would be predicted if the stationary subject were experiencing CW body rotation. Moreover, if the nervous system compensates for Coriolis forces in everyday life, then these compensations should be calibrated to body rotational velocity to move the arm straight to the target because Coriolis forces are proportional to rate of turn. Thus we predict that the magnitude of initial endpoint and curvature errors should be proportional to rate of virtual self-rotation.

As subjects experiencing illusory self rotation make consecutive reaches, we predict a progressive reduction of endpoint and path curvature errors relative to the initial reaches, even when visual and tactile feedback about reaching movements are absent. Such adaptation will be driven by brachial proprio-

ceptors that can signal deviations from the intended movement (Lackner and DiZio 1994). The internal form of this adaptation can be inferred from the pattern of reaches attempted after virtual rotation stops. One extreme form of adaptation is an internal remapping of the relationship between muscle activation and desired body-relative forces. In this scenario, subjects experiencing CCW illusory self-rotation would always plan leftward compensations for anticipated rightward Coriolis forces and would adapt to the resulting leftward reaching errors by reducing the relative activation of muscles pulling left until the brachial feedback signaled the desired trajectory. After virtual rotation stops, these subjects should not program Coriolis force compensations (because they feel stationary) but should underactivate the muscles pulling left because of the internal remapping of muscle activation and desired force. Consequently, they should reach right of their original baseline. Another form of adaptation would involve altering the planned Coriolis force compensation in the context where errors were experienced. If during CCW virtual rotation subjects stop compensating for Coriolis forces normally associated with real CCW self-motion, then when virtual rotation stops they should make straight, accurate reaches on their first attempt because no internal change had been made in motor planning for a nonrotating context.

The first three experiments presented below prove that Coriolis force compensations exist, and that visual information alone about body rotation is sufficient to evoke the appropriate direction and magnitude of compensation. The fourth experiment proves that adaptation of Coriolis force compensation is highly context specific.

EXPERIMENT ONE: CCW ILLUSORY SELF-DISPLACEMENT INDUCED BY CW SCENE ROTATION

METHODS

Subjects

Ten undergraduate students participated. All were right handed and without motor impairments. They were not informed of the hypothesis being tested until completion of the experiment. None had prior experience in reaching experiments. The experimental protocol had been approved by the Brandeis University Committee for the Protection of Human Subjects.

Apparatus

A LEEP Cyberface II head-mounted display (HMD) was used to present visual stimuli to the subject. This HMD has stereoscopic liquid crystal video displays and a lens system providing a binocular field of view 140° horizontal by 110° vertical with ~35° of stereo overlap. It was driven by a LEEP Telehead, which was a stereo video camera platform equipped with a pair of lenses that match the Cyberface II optical system so that the images projected to the subject are orthoscopic. The Telehead was fixed to a desktop surface mounted over the rotation axis of a servo-controlled motor. The edges of the black desktop were marked with yellow tape to provide a stable spatial background for a midline target, a red hemisphere 2 cm diam with a black bull's-eye. The Telehead was angled down to view the desktop and target from a distance of 57 cm. Approximately the upper two-thirds of the Telehead's field of view was the large, rectangular laboratory room in which the rotating table was situated. The room was full of various types of apparatus and had ample spatially distinctive, nonrepetitive characteristics. Our intention was for the Telehead cameras to provide the same image a subject would see if he or she were seated at the desktop looking at the target, with the important exception that the subjects' arms and hands were never in view. Slip rings on the rotator allowed the signals from the Telehead to be fed to the HMD.

The subject sat at a stationary desk to which the HMD was rigidly fixed at the same height and angle as the Telehead on the servo-controlled desktop. Subjects leaned against the facemask of the HMD to stabilize their head and to view the scene transmitted from the Telehead. They never received visual feedback about hand position because the HMD occluded direct sight of the hands and a drape concealed them from the rotating Telehead. They also did not receive tactile feedback about whether the target had been "hit" because there was no physical target on the smooth desktop surface. Figure 2 illustrates the experimental situation and the subject's field of view.

The position of the right, pointing index finger was monitored using a Polhemus 3Space magnetic tracking device. The receiver, which weighs 17 g, was taped to the dorsal tip of the index finger. The Polhemus had an accuracy of 0.8 mm and a resolution of 0.05 mm across the workspace. The measurement coordinate system was adjusted so that its fore-aft axis corresponded to a line drawn between a midline start button near the torso and the perceived position of the visual target. The second axis of the measurement system was aligned with the gravitational vertical.

Procedure

At the start of an experimental session, the HMD was adjusted to accommodate each subject's height, and identical adjustments were made to the Telehead to maintain registration of the real and virtual desktops. Directly verifying co-registration was impossible because the display was not see-through; however, no subject reported an apparent disparity between what he saw in the HMD and felt when running his unseen hand over the desktop. The subject was asked to place his or her right finger at the center of the target seen through the HMD. This was necessary for calibration because differences in how

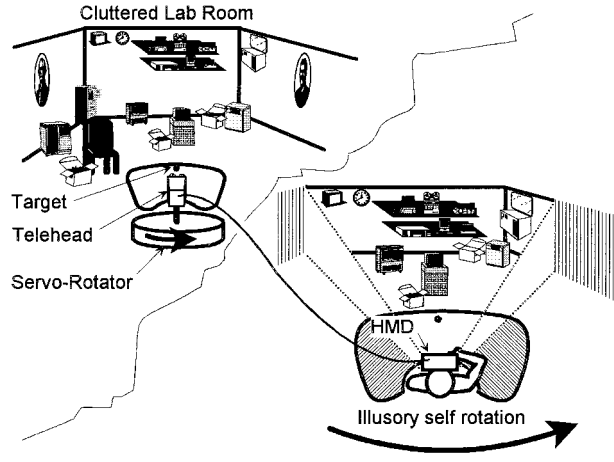

FIG. 2. Experimental setup: subjects sat in a curtained alcove at a smooth, level, stationary desktop. A head-mounted display (HMD) fixed to the desk provided a visual scene generated by a Telehead video camera located on a twin desktop mounted on a servo-rotator in the center of the cluttered laboratory room. A target was located near the outer edge of the servo-controlled desktop. The HMD and Telehead were connected through slip rings. Subjects looking in the HMD saw a real-time image of the Telehead's field of view and perceived themselves to be seated at the desk in the center of the laboratory room, with a midline target on their desk. Subjects received no visual or direct tactile feedback about movement accuracy. Telehead rotation was counterclockwise for *experiments 1, 3,* and *4* and clockwise for *experiment 2.* During Telehead rotation the subjects perceived themselves, the desk, and target as moving in unison relative to the visual background.

the HMD fit the subject could result in small individual variations in the perceived absolute position of the target. On average, the visual target was localized 39 cm from the start button.

The experimental part of a session after calibration was divided into three periods: pre-exposure, exposure to visual motion, and post-exposure. Twenty reaches, in 2 blocks of 10 separated by a 15-s rest period, were made in each period. Subjects lifted their finger from the start button to point at the center of the visual target and reached in a single movement without stopping along the way. The finger contacted the physical desk surface at the end of the reach. The subjects were instructed to make midmovement corrections if they felt they were missing the target but not to stop and start over to do so. Before the start of the experiment, the subjects made several practice reaches until their movement duration was in the 0.5- to 0.75-s range. After completion of a reach, the subject lifted his or her hand up and brought it slowly back to the start button without touching the desk surface.

After a subject completed the 20 pre-exposure reaches, the servotable holding the Telehead was accelerated to 60°/s CCW. This generated a rightwardly moving visual scene in the HMD that caused the subject to experience leftward, CCW self-motion. The desktop viewed by the Telehead appeared to rotate with the subject. After 2 min of constant velocity exposure, the subject was told to begin the exposure period reaching movements. When the 20 per-exposure movements were completed, the Telehead was decelerated to rest. Two minutes were allowed to pass, and then the subject made 20 post-exposure reaching movements to complete the experimental trials. The subjects were then questioned about their experiences of self-motion and self-displacement and visual scene motion during the exposure and post-exposure periods.

Data analysis

The Polhemus signal was sampled at 100 Hz for 1 s after release of the start button. The peak velocity, peak curvature, endpoint, and duration of each pointing movement were calculated by a program that also determined when the finger came to rest. Rest was defined as the location at which the changes in the fore-aft and vertical directions of the index finger position stayed below 35 mm/s for a duration of 40 ms. We used the maximum deviation of the finger from a straight line between the start and endpoint as a measure of trajectory curvature.

Our primary interest was in how the exposure and post-exposure reaches differed relative to the pre-exposure baseline reaches. Baseline for each subject was calculated as the average of the last five pre-exposure reaches. Our analyses focus on the second through fourth per-exposure reaches (where the peak deviations from baseline consistently occurred), the final three per-exposure reaches, and the average of the first three post-exposure reaches.

RESULTS

Pre-exposure

Subjects made nearly straight line reaching movements to the virtual target. The average peak trajectory curvature was 9 mm leftward of the line connecting movement start and end positions. Movement distance averaged 37 cm. Duration averaged 600 ms with a peak velocity of 1,330 mm/s.

Per-exposure

All subjects but one showed leftward deviations of their movement endpoints relative to prerotation. These are illustrated in Fig. 3, *A* and *B*. The peak endpoint deviation occurred on the second, third, or fourth exposure reaches for different subjects. The average endpoint over these three movements, across subjects, was deviated 26 mm left of baseline. Subsequent movement endpoints showed a gradual return toward baseline values. The average of the final three exposure reach endpoints was 14 mm left of baseline. The peak curvature of the per-exposure reaches occurred on the second movement. In accord with how we determined endpoint deviation, we averaged the curvatures of movements 2–4 and obtained a 17-mm leftward deviation, which was 8 mm left of baseline curvature. Successive curvature values for the remaining reaches in the 1st set of 10 reaches hovered below this value. The curvatures of the 2nd set of 10 reaches were generally smaller than those of the 1st, although more variable. The final three reaches

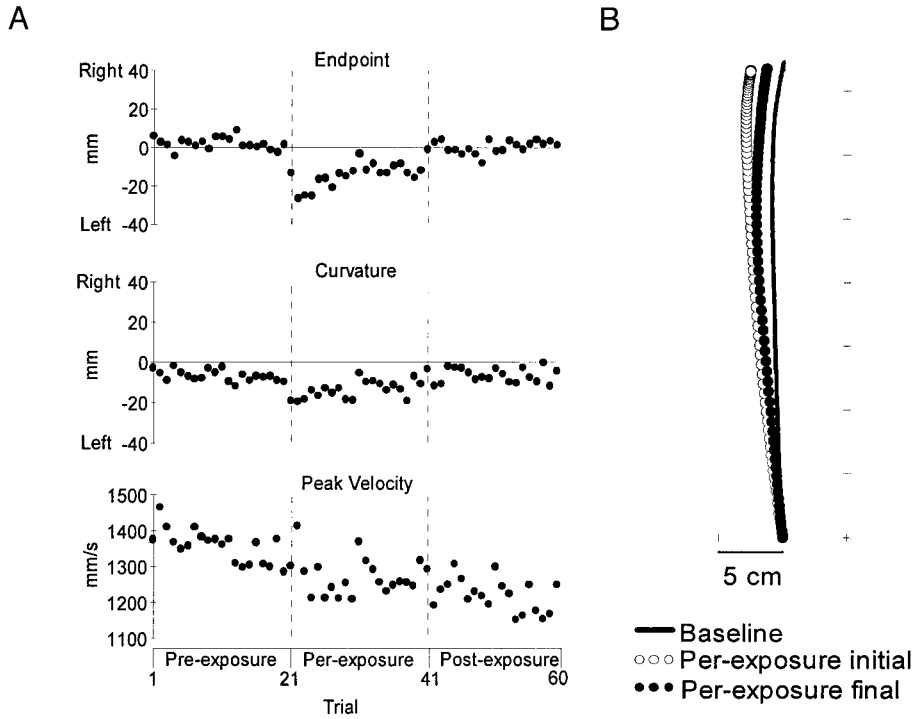

FIG. 3. Results of *experiment 1*. *A*: plots of lateral endpoints, curvatures, and peak velocities, for 20 baseline, 20 per-exposure, and 20 post-exposure reaches, averaged across subjects (n = 10). Dashed vertical lines indicate the initial per-exposure and initial post-exposure reaches. *B*: movement paths in the horizontal plane averaged across 10 subjects. Baseline: average of last 5 pre-exposure reaches. Per-exposure initial error: average of 2nd, 3rd, and 4th per-exposure condition reaches. Per-exposure final: average of the last 3 reaches in per-exposure condition.

showed an average curvature of 3 mm left of baseline values. The average movement durations over the initial and the final three per-exposure reaches were 580 and 620 ms, respectively, whereas the peak velocities for these same trials were 1,335 and 1,300 mm/s, respectively.

All of the subjects experienced leftward illusory self-motion and displacement within a few seconds after onset of exposure to visual motion. They felt as if they and the desk were turning together in relation to a stationary visual room and in relation to external space. This experience remained constant throughout the exposure period. Five of the subjects reported that their initial reaches in the exposure condition were somehow forcibly deviated leftward from their intended path. This sensation attenuated over subsequent reaches. The virtual target did not appear to change its position in relation to the table top for any of the subjects.

Post-exposure

The initial and subsequent reaches were essentially at pre-exposure baseline values, with the average endpoint of the first three reaches lying only 2 mm right of baseline and with an average curvature 1 mm rightward of baseline. This means that when the subjects again felt themselves to be stationary, there were no aftereffects from the prior exposure period. The average movement duration for the initial post-exposure reach was 620 ms, with a peak velocity of 1,270 mm/s. Successive reaches hovered about these values.

Statistical analysis

ENDPOINTS. Using a repeated measures one-way ANOVA, we compared the average endpoints of the baseline (last 5 pre-exposure reaches), per-initial (average of the 2nd, 3rd, and 4th per-exposure reaches), per-final (last 3 per-exposure reaches), and post-initial (1st 3 post-exposure reaches) reaches. The changes from baseline are shown in Fig. 4*A*. We found a highly significant difference between the four values ($P = 0.001$, $F = 7.0$). Post hoc Tukey comparisons ($P < 0.05$ at least) showed that the per-initial mean was significantly displaced from both the baseline mean and the post-initial mean. The per-final endpoint mean was about halfway between the per-initial mean and the baseline, and it did not significantly differ from them. Finally, the baseline and post-initial means did not differ significantly from each other.

PATH CURVATURE. A one-way, repeated measures ANOVA on curvature trials failed to find any significant differences between them. Neither the per-exposure nor the post-exposure measure differed significantly from the pre-exposure baseline.

DISCUSSION

The visual scene of a rotating laboratory room displayed by the Telehead evoked compelling illusory self-rotation and self-displacement in all of our subjects for the duration of the exposure period. Concurrently, the subjects' initial exposure condition reaches exhibited leftward deviated paths and endpoints relative to pre-exposure baseline. On average, beginning with the fourth per-exposure reaching movement, path curvature and endpoint began to return toward pre-exposure baseline. This pattern corresponds to what we predicted would occur if subjects show anticipatory motor compensations for Coriolis forces that never materialize.

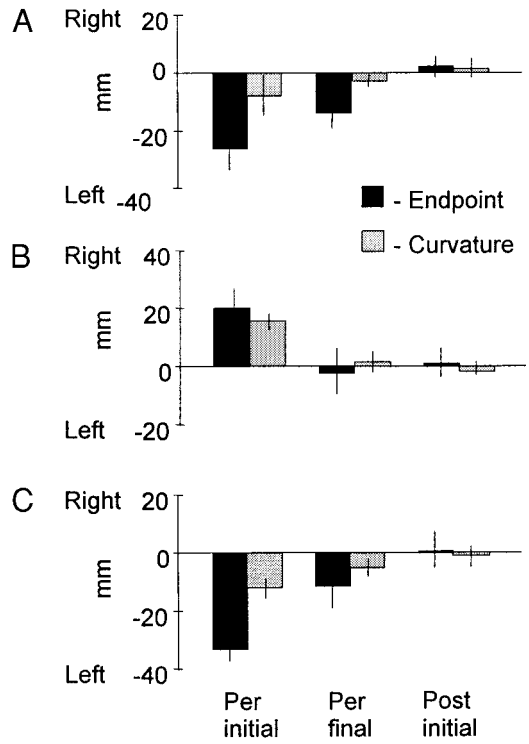

FIG. 4. Per-exposure and post-exposure lateral endpoint and path curvature errors, relative to baseline averaged across subjects for *experiment 1* (*A*): counterclockwise Telehead rotation at 60°/s, 20 per-exposure reaches, $n = 10$; *experiment 2* (*B*): clockwise 60°/s Telehead rotation, 20 per-exposure reaches, $n = 11$; and *experiment 4* (*C*): counterclockwise 60°/s Telehead rotation, 80 per-exposure reaches, $n = 10$. Error bars represent 1 SE. Per-initial endpoint: the average of the 2nd, 3rd, and 4th per-exposure movements; Per-final: the average of the last 3 per-exposure movements; Post-initial: the average of the 1st 3 post-exposure movements.

EXPERIMENT TWO: CLOCKWISE ILLUSORY SELF-DISPLACEMENT

To gauge the reliability of the results from *experiment 1*, we ran subjects with precisely the same conditions but with the direction of visual motion reversed. We predicted that these subjects would experience self-rotation in the opposite direction and show mirror image patterns of exposure condition reaches, both for curvature and endpoint, compared with the subjects of *experiment 1*.

Eleven new subjects participated who were right-handed and without motor impairments. Precisely the same equipment and experimental protocol were used as in the first experiment. The only difference was that the LEEP Telehead unit was rotated CW during the exposure condition to induce the sensation of CW, rightward turning and displacement in the subjects.

RESULTS

Pre-exposure

The subjects made pointing movements that had an average peak curvature of 1 mm rightward of a line connecting the movement start and endpoints. Duration averaged 610 ms, and peak velocity, 1,420 mm/s.

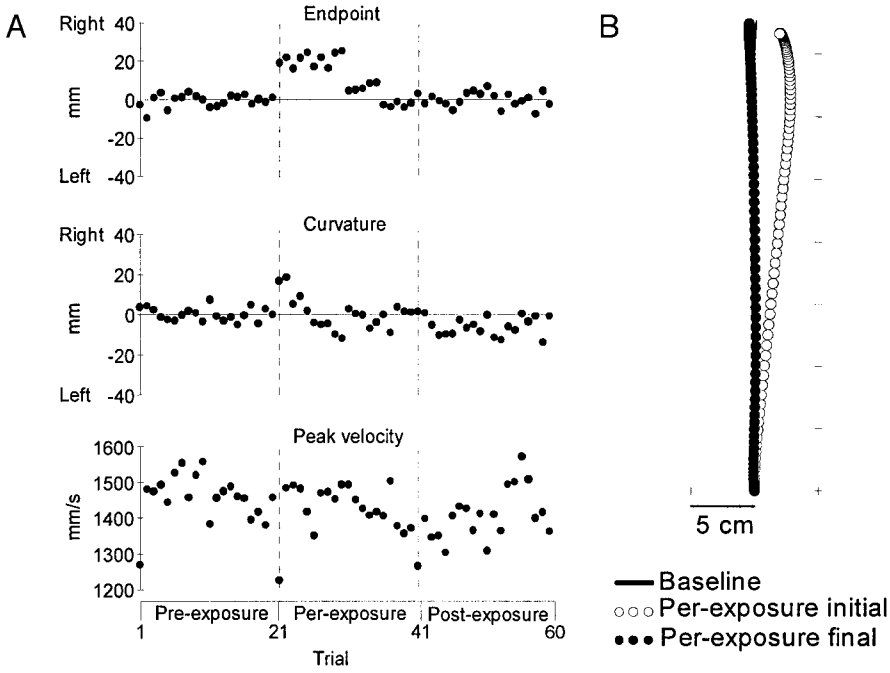

FIG. 5. Results of *experiment 2*. *A*: plots of lateral endpoints, curvatures, and peak velocities, for 20 baseline, 20 per-exposure, and 20 post-exposure reaches, averaged across subjects ($n = 11$). Dashed vertical lines indicate the initial per-exposure and initial post-exposure reaches. *B*: representative movement paths in the horizontal plane averaged across 11 subjects. Baseline: average of last 5 pre-exposure reaches; Per-exposure initial: average of 2nd through 4th per-exposure condition reaches; Per-exposure final: average of last 3 reaches in per-exposure condition.

Per-exposure

The initial per-exposure movements were deviated right of baseline, with the peak endpoint deviation occurring on movements 2, 3, or 4 and peak curvature on the first or second movement for all but one subject. Figure 5, *A* and *B*, illustrates this pattern. As in *experiment 1*, the initial per-exposure endpoint and curvature deviations were computed by averaging movements 2–4. The endpoint deviation was 20 mm rightward of pre-exposure baseline values. After these three reaches, the endpoints maintained roughly the same average deviation for the remainder of the first set. The second set of exposure reaches showed two endpoint plateaus, with the first five reaches all ending at roughly the same point, 5 mm right of baseline. The last five movements of the exposure condition showed a complete return to baseline, with the average of the last three endpoints 2 mm left of baseline. The curvatures of per-exposure reaches 2–4 averaged 16 mm right. The trajectory curvatures gradually diminished, with the final three exposure reaches showing an average curvature of only 1 mm right of baseline values. Movement durations for the initial and final reaches averaged 800 and 670 ms, respectively, whereas the peak velocities for these same movements were 1,490 and 1,370 mm/s, respectively.

All of the subjects experienced clockwise, rotary self-displacement at a constant speed during the exposure period. This sensation began soon after the Telehead began rotating. None of the subjects reported any motion of the target relative to the desk. Seven of the subjects reported feeling a "force" or "tug" deviating their arm rightward from its intended path during their initial reaches. One subject reported slight stomach discomfort, but not strong enough to warrant ending the experiment.

Post-exposure

The endpoints of the initial post-exposure reaches were very close to pre-exposure baseline, with the average of the first three post-exposure endpoints lying only 1 mm rightward of baseline. The postrotation reaches were essentially straight with the average of the first three reaches showing a curvature of only 2 mm leftward of baseline. The average duration of the post-exposure initial movement was 620 ms, with an average peak velocity of 1,360 mm/s.

Statistical analysis

ENDPOINTS. We compared the means of the baseline (last 5 pre-exposure reaches), per-initial (per-exposure reaches 2–4), per-final (last 3 per-exposure reaches), and the post-initial (1st 3 post-exposure reaches) endpoints in a one-way repeated measures ANOVA. The changes from baseline are presented in Fig. 4*B*. The differences between these four means were highly significant ($P = 0.006$, $F = 5.1$). Post hoc Tukey tests showed that the per-initial mean differed significantly from all other means, and that the per-final mean did not differ from either the baseline mean or the post-initial mean. The baseline and post-initial means did not differ from each other.

PATH CURVATURE. A repeated measures one-way ANOVA showed highly significant differences ($P < 0.001$, $F = 7.3$) among the means of the baseline, per-initial and post-initial movements, as defined above. Tukey test comparisons showed that the baseline and per-initial curvature means differed, as did the per-initial and per-final exposure curvatures ($P < 0.05$ at least). As with the endpoints, the baseline, per-final reaches, and the post-initial reaches were not statistically different from one another.

DISCUSSION

Subjects in this experiment experienced the opposite direction of apparent self-rotation and displacement as the subjects of *experiment 1*. The movement paths and endpoints of their initial per-exposure reaches showed a mirror image pattern to the subjects of *experiment 1*, just as we predicted would occur

if compensations were being made for the Coriolis forces usually generated by reaches made during rightward rotation. With subsequent per-exposure reaches, their movements returned to pre-exposure baseline curvature and endpoint values. Adaptation was slightly better in *experiment 2*, perhaps reflecting the mechanical asymmetry of moving the same arm in opposite directions.

EXPERIMENT THREE: VARYING SPEEDS OF ILLUSORY SELF-DISPLACEMENT

The first two experiments demonstrated that compensations for Coriolis forces are automatically planned for the direction of apparent body motion. Our next goal was to assess whether compensations for self-generated Coriolis forces would be graded with the speed of apparent body rotation. We predicted this should occur because Coriolis force magnitude is proportional to angular velocity. Visually induced self-rotation "saturates" as stimulus speed goes above ~60°/s (Dichgans and Brandt 1974). Consequently, compensations for expected but absent Coriolis forces should show a corresponding saturation.

Fifteen individuals who had not been in the earlier experiments consented to participate. They were right-handed and free of motor impairments. The LEEP Telehead unit was rotated CCW to induce CCW, leftward apparent turning and displacement in the subjects, who were divided into groups of three to receive a stimulus speed of either 30, 45, 60, 90, or 120°/s. We were interested only in the magnitude of the initial reaching errors. Each session consisted of 10 baseline reaches, 8 with exposure to visual motion, and 10 after visual motion exposure. No reaches were made in the per- and post-exposure periods until subjects had viewed the rotating or stationary scene, respectively, for 2 min.

RESULTS

When the Telehead was rotating, all subjects experienced compelling illusory CCW self-rotation and displacement of themselves and the desk as a unit in relation to a stationary room. Their initial reaching movements deviated leftward an amount that increased with stimulus speed up to 60°/s. Figure 6 illustrates the reaching endpoints and curvatures, averaged over three subjects per group. During stimulus rotation, the peak leftward deviation always occurred in movements 2, 3, or 4 for different subjects. The endpoints of later reaches returned toward baseline, especially at higher stimulus speeds. Following the procedure of *experiments 1* and *2*, the average of movements 2–4 during stimulus rotation was compared with the average of the last five baseline reaches. Movement endpoints shifted left of baseline 15, 32, 36, 31, and 29 mm during visual stimulation at the five rotation speeds, in order from 30°/s to 120°. The change from baseline is significant in every case (directional *t*-tests with Bonferroni correction, adjusted $P < 0.05$). A linear regression model explained a significant ($P = 0.047$) portion of the increase in leftward deviation as a function of stimulus speeds up to 60°/s. Above 60°/s there was no further increase in endpoint error.

Reaching movements were straight before the scene started rotating and became curved to the left when subjects were viewing the moving virtual scene. The average change from baseline increased monotonically, 6, 12, 19, 22, and 26 mm leftward over the stimulus range from 30 to 120°/s. The deviation from baseline was significant for speeds 60°/s and above (directional *t*-tests with Bonferroni correction, $\alpha = 0.05$). There was a significant ($P = 0.029$) linear regression of curvature on the whole range of stimulus speeds; however, the increase in curvature decreased at higher speeds. Curvature and endpoint tended to decrease toward baseline over the eight movements of each per-rotation period.

DISCUSSION

This experiment shows that the magnitude of automatic compensation for Coriolis force is proportional to the registered speed of rotary self-displacement. Both endpoint and curvature errors increase as the speed of the rotating scene increases up to 60°/s.

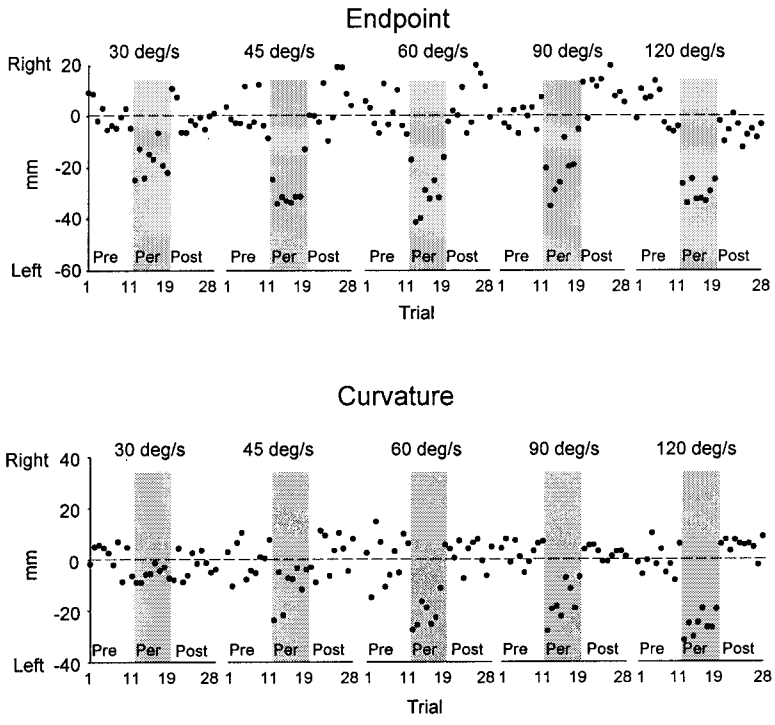

FIG. 6. *Experiment 3*: plots of lateral endpoints and curvatures for 10 baseline, 8 per-exposure, and 10 post-exposure reaches for 5 different per-exposure stimulus angular velocities, $n = 3$ per stimulus. Shaded regions indicate per-exposure reaching endpoints and curvatures.

Above this speed movement curvature increases more slowly and endpoint errors plateau, as predicted.

EXPERIMENT FOUR: 80 REACHES DURING ILLUSORY CCW SELF-DISPLACEMENT

In *experiments 1–3* stationary subjects exposed to rotary scene motion experienced self-rotation and displacement and made reaching errors in the direction opposite the Coriolis forces their voluntary movements would have generated if they had actually been rotating. In a series of 20 reaches, under these exposure conditions, movement endpoints and curvatures returned toward but did not fully attain pre-exposure baseline levels. A striking result from *experiments 1* and *2* was that when exposure to visual scene motion ceased the initial post-exposure reaches were accurate. The form of adaptation acquired per-exposure did not have any consequences that persisted post-exposure. In *experiment 4*, we increased the number of per-exposure reaches from 20 to 80 to elicit a greater degree of adaptation. Ten naive subjects made 8 sets of 10 reaches rather than just 2 sets, for a total of 80 movements during the exposure period involving 60°/s CCW Telehead rotation. We predicted that near complete return to baseline performance would occur and that aftereffects would still be completely absent after the extended opportunity for adaptation.

RESULTS

Pre-exposure

Subjects essentially reached in straight lines to the virtual target. The peak movement curvature was 1 mm, rightward. Peak forward velocity was 1,270 mm/s, with an average movement duration of 650 ms.

Per-exposure

All subjects showed large, initial leftward endpoint and curvature errors, relative to baseline values. The characteristics of all movements are illustrated in Fig. 7. For individual subjects, the peak endpoint deviation occurred in the second or third per-exposure reach, and the peak curvature occurred on the first. However, our quantitative analyses of initial per-rotation endpoint and curvature are based on averages of movements 2–4, as in prior experiments. The initial endpoint deviation was 29 mm left of baseline. Subsequent movements gradually returned toward baseline, with the last three exposure reaches ending 11 mm left of the pre-exposure position. The initial trajectory curvature was 11 mm left of a line drawn between the start and end positions of the movement. With successive reaches, curvature values approached baseline, with the final three movements showing an average curvature of 4 mm left of the baseline patterns. The average movement duration of the initial and final per-exposure reaches was each 660 ms. The peak forward velocities for these reaches were 1,280 and 1,270 mm/s.

All subjects experienced strong illusory self-rotation and displacement immediately after stimulus onset. They reported feeling that they and the desk were moving in unison CCW (leftward) in a stationary room. This sensation did not fluctuate throughout the course of the 80 exposure reaches. Four subjects reported that their initial per-exposure reaches felt pulled off to the left by an external "force," this sensation abated with additional reaches. Three subjects reported feeling slightly dizzy during the course of exposure to visual motion but not enough to impair their reaching ability.

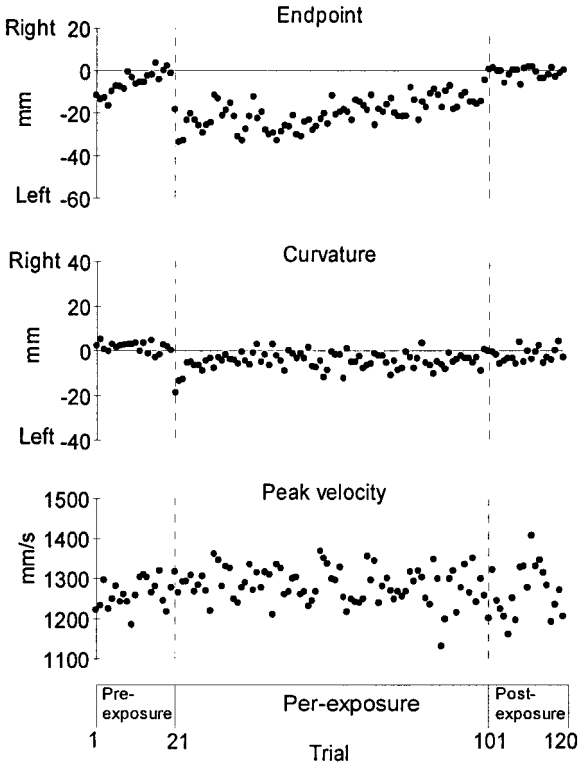

FIG. 7. *Experiment 4*: plots of lateral endpoints, curvatures, and peak velocities, for 20 baseline, 80 per-exposure, and 20 post-exposure reaches, averaged across subjects ($n = 10$). Dashed vertical lines indicate the initial per-exposure and initial post-exposure reaches.

Post-exposure

The initial three post-exposure reaches were essentially identical to baseline. Reaches on average ended 1 mm right of baseline, with a curvature of 1 mm leftward. None of the subsequent movements deviated from baseline either. The average movement duration was 660 ms, with a peak forward velocity of 1,260 mm/s. None of the subjects reported visual or postural aftereffects as a result of exposure to scene motion. Three subjects reported feeling slightly motion sick but not at a level to necessitate premature termination of the experiment.

Statistical analysis

A repeated measures ANOVA comparing the means of the pre-exposure baseline, the per-initial, per-final, and the post-initial endpoints was highly significant ($P < 0.001$, $F = 25.0$). The changes from baseline are represented in Fig. 4*C*. Tukey comparisons ($P < 0.05$) between these values showed that per-initial differed from both pre-exposure baseline and per-final, whereas pre-exposure baseline did not differ from per-final and post-initial. The same pattern and statistical differences were found for movement curvature.

DISCUSSION

Eighty reaches made by subjects during exposure to 60°/s CW scene motion led to complete adaptation of movement curvature:

the movement paths of the final exposure condition reaches were statistically indistinguishable from pre-exposure baseline. Movement endpoints showed virtually complete adaptation as predicted: the endpoints of the final per-exposure reaches were not significantly different from per-exposure baseline. Post-exposure there were no aftereffects. This means that the adaptive changes in control of reaching instituted during prolonged exposure to apparent self-displacement are context specific and affect motor control only in situations where rotary self-motion is the same as when reaching errors were experienced.

GENERAL DISCUSSION

Coriolis forces are present during most natural multijoint movements. If the shoulders are rotating, either actively or passively, and a reaching movement is made, then Coriolis forces proportional to rotation rate and reaching velocity will be generated orthogonal to the forward movement of the hand and arm. Although Coriolis forces are lawfully related to the physical context of arm and body motion, we have performed a series of experiments uncoupling the relationship between the Coriolis forces and the sensory information about the context in which they occur. For example, a subject seated passively at the center of a fully enclosed room rotating at constant velocity feels stationary because the available sensory information is the same as would be present if he or she were stationary. However, the actual rotation governs the Coriolis forces generated by movements, and large reaching errors result, in the direction of those forces (Lackner and DiZio 1994). Such errors mean that the CNS's mode of executing the planned trajectory is not adequate to eliminate deviations due to unexpected Coriolis force perturbations. This finding strongly contradicts the equifinality prediction of equilibrium point hypotheses (Bizzi et al. 1992; Feldman 1986). These theories predict that transient perturbations of movement paths will not affect the endpoints of the movements and that Coriolis compensations need not be planned. The experiments reported here prove that Coriolis compensations are planned and begin to elucidate the nature of that planning.

We showed that stationary subjects experiencing body rotation make predictable patterns of errors in pointing to visual targets. We predicted that stationary subjects experiencing leftward turning would compensate for the Coriolis forces of a forthcoming reaching movement by generating greater leftward joint torques than when they feel stationary and as a consequence make endpoint errors to the left because no Coriolis forces are actually present. The Coriolis forces generated by reaching movements during real angular displacement of the torso have a bell-shaped profile because they are proportional to the limb's linear velocity, which has a bell-shaped curve (Morasso 1981). If compensations are centrally implemented to retain the normal straight line shape of hand trajectory (relative to the trunk) as well as to achieve the desired endpoint, then movements made during leftward illusory self-motion should be curved with a maximum leftward deviation roughly mid-movement. Subjects experiencing illusory rotation and displacement in fact made reaching movements with curvature and endpoint deviation in the direction opposite the Coriolis forces that would have been present if they had really been rotating. The presence of the predicted endpoint and curvature errors during virtual self-rotation supports the existence of automatic Coriolis force compensations. The generation of curved movements indicates that there is an internal compensation for the Coriolis force profile of the entire trajectory of a forthcoming movement, not just the endpoint. In other words, compensatory forces are generated at each moment that balance the inertial forces associated with the arm's planned linear velocity and the body's registered angular velocity. This process operates also in a natural environment whenever the torso is actively turning during a reach.

Subjects experiencing illusory CW self-rotation (*experiment 2*) showed exactly the opposite pattern of the subjects in *experiment 1*, who experienced CCW rotation. In *experiment 3*, subjects experiencing different speeds of illusory self-rotation made endpoint and curvature errors whose magnitudes were proportional to their perceived rate of turning. These direction- and speed-specific errors show that detailed sensory representations of spatial context are taken into account in planning reaching movements. Compensations for Coriolis forces associated with self-motion are unconscious, pre-programmed, directionally appropriate, and proportional to perceived self-rotation speed.

The adaptive reduction of endpoint and curvature errors with successive reaches during illusory self-rotation are important for two reasons. First, they indicate that a combination of brachial proprioceptive afferent signals and efferent monitoring is sufficient for subjects to detect when their reaches deviate from the intended path and terminus and to activate an incremental, adaptive reduction of the deviations. Second, the presence of adaptation also shows that the errors produced during visually induced illusory self-rotation are not caused by visual mislocalization of the target.[2]

When subjects were again reaching accurately after many movements during illusory self-rotation, they must have been generating different motor commands than when they were first exposed, because the real force background had not changed. Adaptation did not involve a change in internal registration of self-motion because experienced self-motion remained constant during the exposure period. The adaptive change that occurred was automatic and unconscious yet had no consequences when the subjects were no longer experiencing self-rotation. For example, in *experiment 4* subjects achieved complete adaptation of movement curvature and substantial endpoint adaptation in 80 reaching movements yet showed no aftereffects at all. One internal change that could explain these results is generation of a new estimate of the magnitude of Coriolis forces associated with reaching velocity and self-rotation speed. During virtual rotation, subjects initially compensated for the Coriolis forces that would have been physically associated with real self-motion. If adaptation involved learning to generate no compensation during apparent self-motion, then they should immediately be able to make straight, accurate reaches when they are no longer experiencing

[2] A small visual target can be mislocalized when it is presented against a moving visual background (Duncker 1938). We were concerned about the elicitation of such a mislocalization because, if present, it would be in the direction of the endpoint errors predicted in our experiments. The target used in the present study was presented on a desktop with distinctly marked borders because such borders minimize or eliminate target mislocalizations. We have shown elsewhere that when visual mislocalizations (but not illusory self-rotation) are intentionally induced, subjects in pointing without sight of their hands, move in straight lines to the wrong place, over subsequent reaches continue pointing straight to the same wrong place and always feel that their arms have carried out the intended movements (Cohn et al. 1996).

virtual rotation because no internal change had been made in the planned compensation for non-rotating conditions.

Such context-specific adaptation to Coriolis forces is consistent with the results of our SRR experiments, where powerful mirror-image aftereffects are generated when adaptation to physical Coriolis forces has been achieved and subjects again reach while physically stationary. In the SRR experiments, the subjects always felt stationary. To deny information about rotation, we had accelerated them on-axis in the fully enclosed SRR at below threshold rates for detection of rotation, kept them at a constant angular velocity, and then decelerated them to rest at below detection threshold rates (Lackner and DiZio 1994). Subjects in this situation initially plan no correction for Coriolis forces because they feel stationary, and none are necessary when they are stationary. Consequently, during rotation, their initial movements are deviated in the direction of the Coriolis forces. With successive reaches, movement planning is progressively adapted to reduce the errors detected on the basis of brachial proprioceptive and efferent signals and somatosensory signals. The new plan involves correcting for Coriolis forces in a registered non-rotating context. When the SRR stops, the registered context is still "no rotation," but now Coriolis forces are absent when the subject reaches. Consequently, the subjects' initial post-rotation reaches are mirror images of their initial per-rotation reaches because they are still compensating for the Coriolis forces expected during "non-rotation."

The occurrence of context-specific compensations for Coriolis forces in our virtual rotation paradigm demonstrates that the CNS partitions the net force field for a movement into functionally significant components, including self-generated accelerative forces, and simultaneously maintains the ability to generate separate representations of the different components. Previous research has shown that people can adapt to novel gravitoinertial (Cohen 1970; Fisk et al. 1993) and local contact (Sainberg et al. 1993; Shadmehr and Mussa-Ivaldi 1994) force fields. For example, a viscous force field produced by a robotic manipulandum initially deviates movements, but subjects can adapt with hundreds of practice trials (Shadmehr and Mussa-Ivaldi 1994). If subjects are exposed to a second, conflicting force field within a critical period, their adaptation to the first is lost (Brashers-Krug et al. 1996). We think that context-specific adaptation does not occur in this situation because the only contextual cue is the contact force on the hand resulting from the force field itself. The proper motor compensation to use can only be recognized by moving the manipulandum and sensing its response. By contrast, we have demonstrated here that for a free reaching movement the nervous system continually monitors the context of body motion and can generate an internal model of the Coriolis force expected throughout the entire trajectory of a forthcoming movement. Furthermore, motor adaptation can be retained simultaneously for a rotating and a non-rotating context.

A model of how the CNS may incorporate an internal model of Coriolis forces into movement plans is presented in the shaded part of Fig. 8. The brain generates separate internal models of different components of the entire load, such as contacting forces (e.g., movable objects, mechanical devices, support surfaces) versus non-contacting external (e.g., gravity) and internal (e.g., Coriolis and inertial) influences. A Coriolis force field representation, F_{Cor}, is generated based on a representation of the body rotation expected during the reach, ω, which can be constructed from a summation of the sensed motion of the body before the reach and the planned motion of the body during the reach. Sensed motion before the reach is signaled by the visual, vestibular, and somatic touch, pressure and kinesthetic (TPK) systems; representations of desired body and arm trajectory are present at an early stage in the generation of natural reaching movements. The arm trajectory plan and the internal Coriolis force field model enter an execution control transformation to generate a muscle activation profile.

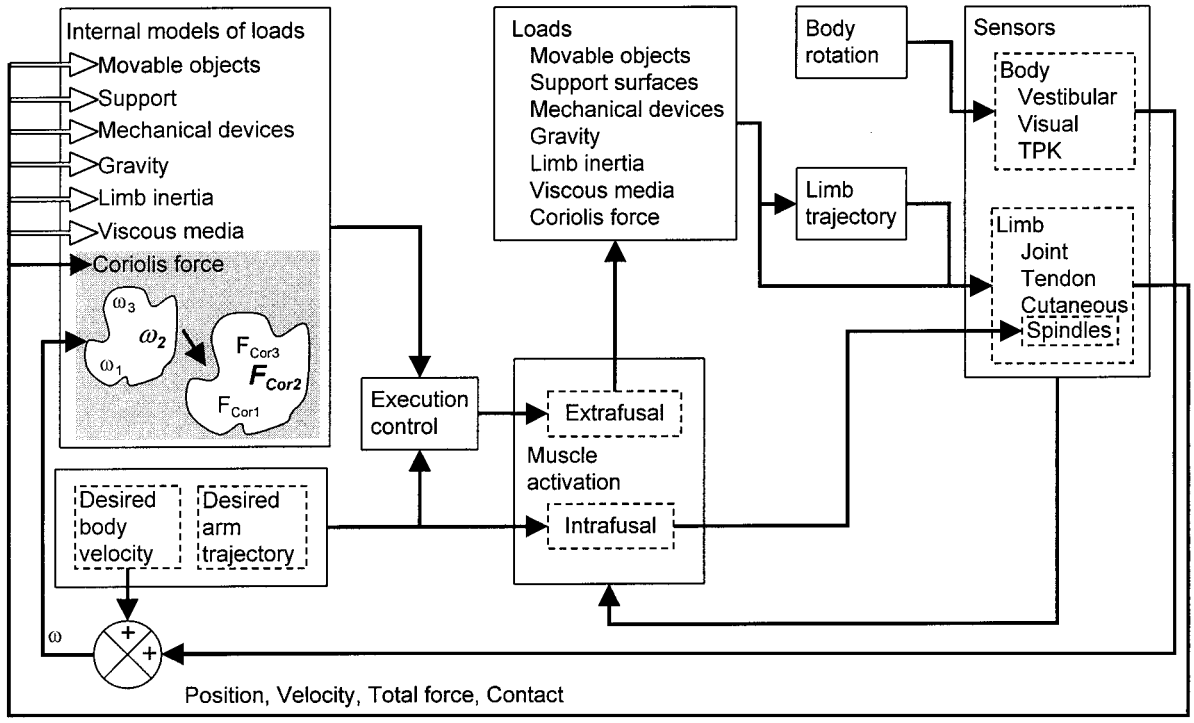

FIG. 8. Model of compensation of reaching movement for self-generated Coriolis forces. See text for explanation.

(This process is also influenced by internal estimates of non-Coriolis loads.) The muscle forces interact with actual loads to generate a reaching movement. Brachial cutaneous, joint, tendon, and spindle receptor feedback are used to detect differences between the actual and desired movement patterns and to drive the adaptive process.

The present model embodies the idea that error detection involves efferent intrafusal and extrafusal signals, although forward models acting on extrafusal commands are also possible (Miall and Wolpert 1996; Wolpert 1997). The brain can recognize whether an unexpected Coriolis force is responsible for the error because only an incorrect internal Coriolis force model will result in velocity-dependent reaching errors in the absence of any tangible contacting force on the limb. Recognition of a Coriolis force perturbation triggers adaptation only of the estimate of the Coriolis force compensation (symbolized by a solid arrow from feedback to the shaded part of the internal model) and not of other internal model components (open arrows). [A previous model (DiZio and Lackner 1995; Lackner and DiZio 1994) showed how terminal versus continuous brachial feedback can selectively initiate adaptation of movement endpoint or trajectory curvature.] This mechanism captures the tendency of the nervous system to make the minimum adaptive changes necessary for reducing errors in the exposure condition and avoiding maladaptive overgeneralization to other tasks or conditions (cf. Lackner 1981). A major feature of this model is that the presence of an error causes adaptive modification only of the Coriolis force compensation generated for the body angular velocity registered at the time of the error, denoted with bold characters in the shaded region of the model. The adaptive change occurs in the generative transformation from ω to $F_{\mathrm{Cor.}}$ Thus context-specific adaptation does not require the implausible postulation of multiple, semipermanent Coriolis force field representations.

In summary, we have shown that Coriolis forces are an important part of the entire physical load during reaching movements in a natural environment, and in both real and virtual rotating environments. The nervous system maintains an internal model of expected Coriolis forces that is used for compensating the entire trajectory of reaching movements, in a generative manner. Information about body rotation is taken into account in programming Coriolis compensations; visual information about body motion alone is sufficient to elicit graded, directionally appropriate compensations. The process for generating Coriolis force compensations can be adaptively modified in a context-specific manner. The level of detailed internal representation of limb movement trajectory in our model also allows for context-specific adaptation to mechanical loads (robotic manipulanda), visual displacement of target arrays or of the hand, and altered inertial loading of the arm.

We thank Y. Altshuler and J. Ventura for technical assistance.

This work was supported by National Aeronautics and Space Administration Grants NAGW-4733, NAGW-4374, and NAGW-4375.

Address for reprint requests: P. DiZio, Ashton Graybiel Spatial Orientation Laboratory, Brandeis University, MS-033, Waltham, MA 02454-9110.

Received 18 March 1999; accepted in final form 8 February 2000.

REFERENCES

BIZZI E, HOGAN N, MUSSA-IVALDI FA, AND GISZTER S. Does the nervous system use equilibrium point control to guide single and multiple joint movements? *Behav Brain Sci* 15: 603–613, 1992.

BORTOLAMI SB, PIGEON P, LACKNER JR, AND DIZIO P. Self-generated Coriolis forces on the arm during natural turning and reaching movements. *Soc Neurosci Abstr* 25: 1912, 1999.

BRASHERS-KRUG T, SHADMEHR R, AND BIZZI E. Consolidation in human motor memory. *Nature* 382: 252–255, 1996.

COHEN MM. Sensory-motor adaptation and after-effects of exposure to increased gravitational forces. *Aerospace Med* 41: 318–322, 1970.

COHN JV, DIZIO P, AND LACKNER JR. Reaching movements during illusory self-rotation show compensation for expected Coriolis forces. *Soc Neurosci Abstr* 22: 426, 1996.

DICHGANS J AND BRANDT TH. The psychophysics of visually induced perception of self-motion and tilt. In*: The Neurosciences,* edited by Schmidt FO and Worden FG. Cambridge, MA: MIT Press, 1974, vol. 3, p. 123–129.

DIZIO P AND LACKNER JR. Motor adaptation to Coriolis force perturbations of reaching movements: endpoint but not trajectory adaptation transfers to the non-exposed arm. *J Neurophysiol* 74: 1787–1792, 1995.

DUNCKER K. Induced motion. In: *A Source Book of Gestalt Psychology,* edited by Ellis WD. New York: Humanities, 1938, p. 161–172.

FELDMAN AG. Once more for the equilibrium point hypothesis (λ model). *J Mot Behav* 18: 17–54, 1986.

FISK J, LACKNER JR, AND DIZIO P. Gravitoinertial force level influences arm movement control. *J Neurophysiol* 69: 504–511, 1993.

HOWARD IP AND CHILDERSON L. The contribution of motion, the visual frame and visual polarity to sensation of body tilt. *Perception* 23: 753–762, 1994.

LACKNER JR. Some aspects of sensory-motor control and adaptation in man. In: *Intersensory Perception and Sensory Integration,* edited by Walk RD and Pick HL. NY: Plenum, 1981, p. 143–173.

LACKNER JR AND DIZIO P. Rapid adaptation to Coriolis force perturbations of arm trajectory. *J Neurophysiol* 72: 299–313, 1994.

MIALL RC AND WOLPERT DM. Forward models for physiological motor control. *Neural Networks* 9: 1265–1279, 1996.

MORASSO P. Spatial control of arm movements. *Exp Brain Res* 42: 223–227, 1981.

PIGEON P, BORTOLAMI SB, DIZIO P, AND LACKNER JR. Arm reaching movements during voluntary trunk rotation involve compensation for self-generated Coriolis forces. *Soc Neurosci Abstr* 25: 1912, 1999.

SAINBERG RL, POIZNER H, AND GHEZ C. Loss of proprioception produces deficits in interjoint coordination. *J Neurophysiol* 70: 2136–2147, 1993.

SHADMEHR R AND MUSSA-IVALDI FA. Adaptive representation of dynamics during learning of a motor task. *J Neurosci* 14: 3208–3224, 1994.

WOLPERT DM. Computational approaches to motor control. *Trends Cognit Sci* 1: 209–216, 1997.